

## EFFECT OF UNINTENDED MAT FOUNDATION INCLINATION ON LOW-COST PVC 'SAND-WICH' BASE-ISOLATION SYSTEM

Z. Zhang<sup>1</sup>, N. Alexander<sup>2</sup> & A. Sextos<sup>3</sup>

<sup>1</sup> University of Southampton, Southampton, UK, [ziliang.zhang@soton.ac.uk](mailto:ziliang.zhang@soton.ac.uk)

<sup>2</sup> University of Bristol, Bristol, UK

<sup>3</sup> University of Bristol, Bristol, UK & National Technical University of Athens, Athens, Greece

**Abstract:** *This work investigates the influence of a sloping seismic base-isolation interface, caused by unintended or mismanaged construction works, on the performance of the low-tech, low-cost PVC 'sand-wich' (PVC-s) base-isolation system developed by the University of Bristol. The motivation for this study is the fact that the sliding characteristics of the PVC-s system may be affected by the inclination of its sliding interface, due to two mechanisms: (a) the reduction or increase of the sliding forces along the downward/upward direction of the slope, respectively, caused by gravity action and (b) the intensified variation of normal contact force on the isolation interface during earthquakes, as a result of the simultaneous action of both the horizontal and vertical accelerations. A probabilistic framework of Incremental Dynamic Analysis (IDA) is setup using a three-dimensional finite-element model of a PVC-s base-isolated school building to statistically study the above effect. Given limited allowance of unintended mat foundation inclination that varies from 0 ° to 3 °, its influence on the effectiveness of the PVC-s system is explored. The results indicate that the isolation interface inclination does not necessarily reduce nor increase the effectiveness of the PVC-s system. On the other hand, maximum and residual sliding displacements can be prominently affected. As the inclination angle increases, the maximum sliding displacement tends to increase as well. At the maximum investigated value of 3 ° inclination, maximum foundation sliding displacement can be factored by 2.5 to that of the flat-ground case, which is in line with engineering judgement. The residual-to-maxima sliding displacement ratio also gets closer to unity, meaning that the base-isolated building is less likely to slide upward the slope as inclination angle increases, again in line with intuition. Considering that controlling sliding displacement is not a primary concern in the typical usage scenario of PVC-s system, it is concluded that a potential accidental inclination of the underlying mat foundation is not undermining the effectiveness of this low-cost seismic isolation technology.*

### 1 Introduction

A low-cost, low-tech, sliding-type seismic base-isolation system, termed PVC 'sand-wich' (PVC-s), was recently designed at the University of Bristol. Proof-of-concept large-scale shaking table tests were conducted on the University of Bristol 3 m by 3 m shaking table for prototype PVC-s systems utilising near-rigid steel (Tsiavos *et al.*, 2020) and masonry (Tsiavos, Sextos, Stavridis, Dietz, Dihoru, Di Michele, *et al.*, 2021) superstructure specimens. These pioneering works highlighted that the intended initiation of a dynamic sliding-rolling mechanism of sand particles encapsulated between two hard PVC sheets, covering the full area underneath the building's reinforced concrete mat foundation, can be an effective base-isolation mechanism. Those studies also experimentally evaluated the effective friction coefficient of the PVC-s base-isolation

interface, established the optimal PVC-s system configuration, and proposed construction method for the PVC-sand-PVC profile. A 'hybrid design' approach was also proposed in association with the PVC-s base-isolation system, of which the purpose was to encourage a 'good practice' design for typical low-rise structures in a practical and economical way (Tsiavos *et al.*, 2020; Giordano *et al.*, 2021; Tsiavos, Sextos, Stavridis, Dietz, Dihoru, Di Michele, *et al.*, 2021). Alternative sliding layers such as sand-rubber mixtures (Tsiavos *et al.*, 2019) and various types of rollers (Tsiavos, Sextos, Stavridis, Dietz, Dihoru and Alexander, 2021) were also investigated, which gain improved sliding performance of the base-isolation layer at the cost of higher expenses.

Following the proof-of-concept shaking table tests conducted for prototype PVC-s systems, experimental observations were extended by numerical and statistical simulations on a realistic case of a reinforced concrete school building in rural Nepal, which probabilistically verified the effectiveness of the PVC-s system for the case study school building (Sextos, Zhang and Alexander, 2022). It was considered that the concept of a low-cost sliding foundation system should only be implemented, within a developing country context, as an additional layer of earthquake-proof mechanism to that of a conventional ductile building, which is capacity designed as normal. This is a scenario that can be faced in many parts of the world where there has no specific code provisions for seismic base-isolation of buildings. In such circumstances, the coupling between the nonlinear responses of a sliding foundation together with a yielding oscillator, which is still disputable in the literature (Kikuchi, Black and Aiken, 2008; Vassiliou, Tsiavos and Stojadinović, 2013), was investigated first analytically by solving the Equation of Motion of a simplified PVC-s base-isolated building system, then numerically through a probabilistic framework of Incremental Dynamic Analysis (IDA) (Vamvatsikos and Cornell, 2002). Given the condition that the school building is adequately designed as a ductile earthquake resistant structure according to local seismic code, the effectiveness of the low-cost PVC-s base-isolation system was verified probabilistically for ground motion intensities up to three times the design-level. Additionally, results confirmed that the inclusion of the PVC-s system is always beneficial regardless of the probable variation on sliding interface friction and building ductility levels.

Notwithstanding the above accomplishments, it must be ascertained that the presence of the PVC-s base-isolation system will not worsen the school building's seismic performance in anyway due to potential unsatisfactory quality control or mismanagement during construction. Unintended mat foundation inclination is considered to be a critical construction defect that can be an immediate cause to alter the dynamic properties of a PVC-s base-isolated building. During construction, it is required to carve out a level ground on a non-flat site so to subsequently create a flat base of stabilised soil, upon which the sliding interface of the PVC-s system and the reinforced concrete mat foundation of the superstructure can be built. Poor control of the levelness of the stabilised soil may result in unintended mat foundation inclination, i.e., a sloping base-isolation interface, which can affect the sliding characteristics of the PVC-s system hence the seismic performance of the structure.

Along these lines, the objective of this paper is to probabilistically verify the effectiveness of the PVC-s base-isolation system considering the presence of foundation construction defect, i.e., unintended mat foundation inclination. The study focuses on typical school buildings in rural Nepal as they have specific layouts and consist of an important portfolio of infrastructure. The results are comparatively presented against a PVC-s base-isolated building with perfectly level base-isolation interface, as well as their non-base-isolated counterpart.

## **2 Probabilistic analysis of a PVC-s base-isolated building with unintended ground inclination**

### **2.1 PVC-s base-isolated system and the case study building**

The low-cost PVC-s base-isolation system is illustrated in Figure 1. The fundamental design configuration entails the encapsulation of a predetermined amount of sand grains between two hard PVC sheets, positioned below a reinforced concrete mat foundation of the structure. The encapsulation of sand facilitates a sliding behaviour of the top PVC sheet against the bottom PVC sheet, enhanced by the low rolling resistance of the sand particles (Tsiavos *et al.*, 2020). The robustness of the PVC-s base-isolation strategy is therefore supposedly supported by two mechanisms: Below the sliding threshold, conventional seismic design protects the structure through strength and ductility. If the sliding threshold is exceeded, the initiation of foundation

sliding sets an upper bound in the acceleration transmitted to the superstructure, as illustrated by results from previous proof-of-concept shaking table tests (Tsiavos, Sextos, Stavridis, Dietz, Dihoru, Di Michele, *et al.*, 2021). A gap exists between the edges of the mat foundation and a parapet wall reserved for mat foundation sliding. The parapet wall is designed as a sacrificial element, whose presence is mainly to protect the PVC-s base-isolation interface from daily wear and does not resist to sliding in case of a larger earthquake.

Following the authors' previous study (Sextos, Zhang and Alexander, 2022), the building investigated in the present paper employs the architectural layout of a typical rural Nepalese school building typology, commonly constructed after the devastating Mw 7.8 Gorkha earthquake in 2015. The school building has two storeys for classrooms and a third storey for the staircase accessing the roof area (Figure 2). The building is designed as a standard ductile earthquake resistant structure according to the Nepalese seismic code (National Reconstruction Authority, 2020), employing structural ductility equivalent to Eurocode 8 behaviour factor  $q = 6.0$  (CEN, 2004). The fixed-base fundamental period of the school building was approximately 0.36 s in both the horizontal directions and its total weight, including the raft foundation above the PVC-s isolation interface, is approximately 3,200 kN.

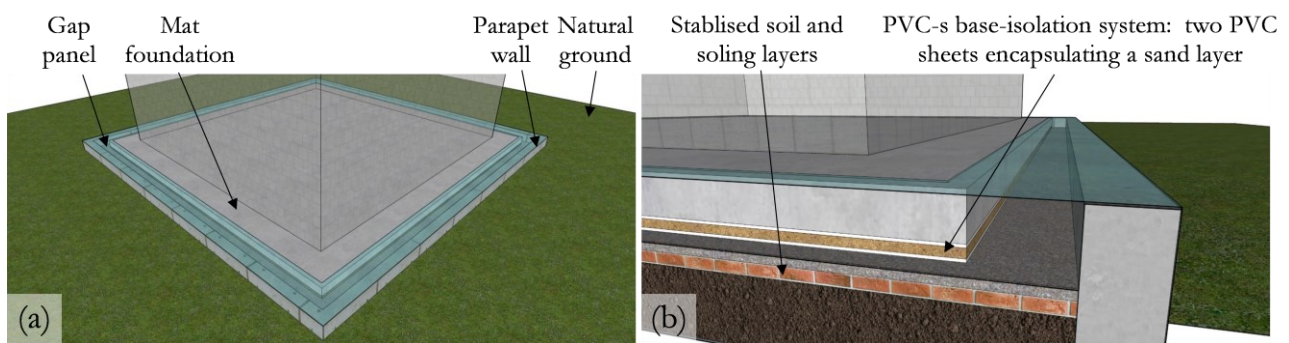


Figure 1: Illustration of the low-cost PVC 'sand-wich' (PVC-s) seismic base-isolation system: (a) overview, (b) sectioned details. Note that the sand layer illustration in the figure is not to scale.

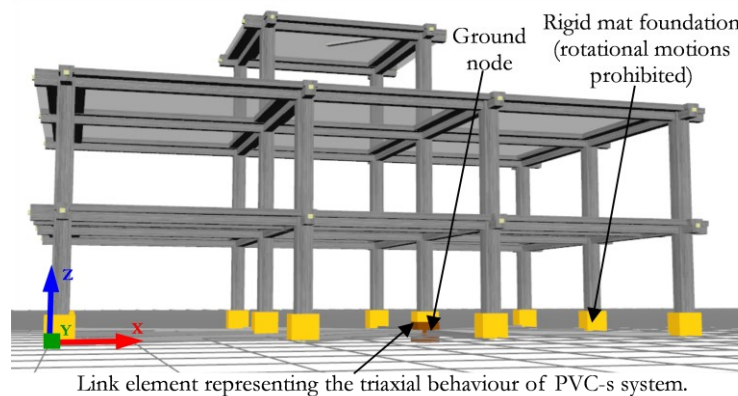


Figure 2: Three-dimensional finite element (FE) model of the case study PVC-s base-isolated school building.

## 2.2 Finite element model implementation

Three-dimensional nonlinear finite-element representation of the studied PVC-s base-isolated school building is modelled using the earthquake engineering finite-element software SeismoStruct (Seismosoft Ltd., 2022) (Figure 2). The reinforced concrete superstructure, having a behaviour factor  $q = 6.0$ , is modelled inelastically employing force-based plastic hinge frame elements and fibre sections. The mat foundation of the school building is assumed rigid and is represented by constraining the bottom nodes of the 12 first-storey columns using a 6-degree-of-freedom (DOF) rigid-link. The mat foundation is then linked to the ground node via a constitutive model describing the 3-DOF translational behaviour of the PVC-sand-PVC seismic base-isolation interface. The equivalent frictional coefficient  $\mu$  of the sliding interface is assumed to be 0.2, in line with previous experimental observations for prototype PVC-s systems (Tsiavos *et al.*, 2020). A more detailed description of finite-element model implementation can be found in (Sextos, Zhang and Alexander, 2022).

The modelling of unintended mat foundation inclination is illustrated in Figure 3. It is assumed that the inclination of the PVC-s base-isolation interface is on x-axis only and can be described using a single parameter, inclination angle  $\theta$ . A positive value of  $\theta$  indicates the ground inclination is sloping down the negative x-direction. When  $\theta$  is non-zero, the known gravity force  $G$  of the building, including the mat foundation, can be decomposed into two components,  $G_x$  and  $G_z$ , one parallel and the other perpendicular to the PVC-s base-isolation interface.  $G_x$  becomes part of the driving force to initiate sliding, whereas  $G_z$  is the new normal force that creates frictional resistance on the PVC-s base-isolation interface. Similarly, the known horizontal earthquake force  $F_h$  at any moment can be decomposed into  $F_{hx}$  and  $F_{hz}$ , and the known vertical earthquake force  $F_v$  into  $F_{vx}$  and  $F_{vz}$ . Given that the inclination angle  $\theta$  due to unintended or mismanaged construction works is unlikely to be larger than  $3^\circ$ , three different levels of  $\theta$  are considered in this study:  $\theta = 1^\circ$  representing moderate mat foundation inclination,  $\theta = 2^\circ$  representing significant mat foundation inclination, and  $\theta = 3^\circ$  representing extreme mat foundation inclination. It is noted that even for the extreme case of  $\theta = 3^\circ$ ,  $\cos(\theta = 3^\circ) \approx 0.9986$  still very closely approximate unity. It is therefore possible to simplify the finite-element modelling of unintended mat foundation inclination: Instead of explicitly model the inclined ground as well as the sloping PVC-s base-isolation interface, the base-isolation interface is modelled as normal (i.e., level to the flat ground) but simulated using adjusted input forces. The adjusted input forces, based on the adjusted coordinate system  $x'-z'$  as illustrated in Figure 3, are calculated as follows:

$$-G_{x'} = -G_x = -G \cdot \sin(\theta) \quad (1)$$

$$-G_{z'} = -G_z = -G \cdot \cos(\theta) \approx -G \quad (2)$$

$$F_{hx'} = F_{hx} = F_h \cdot \cos(\theta) \approx F_h \quad (3)$$

$$F_{hz'} = F_{hz} = F_h \cdot \sin(\theta) \quad (4)$$

$$F_{vx'} = F_{vx} = F_v \cdot \sin(\theta) \quad (5)$$

$$F_{vz'} = F_{vz} = F_v \cdot \cos(\theta) \approx F_v \quad (6)$$

where  $\theta$  is the mat foundation inclination angle, taking values of  $0^\circ$ ,  $1^\circ$ ,  $2^\circ$ , or  $3^\circ$ ;  $G_{x'}$  and  $G_{z'}$  are the forces parallel and normal to the PVC-s base-isolation interface induced by the total gravity force  $G$ ;  $F_{hx'}$  and  $F_{hz'}$  are the forces parallel and normal to the PVC-s base-isolation interface induced by the horizontal ground motion action  $F_h$ ;  $F_{vx'}$  and  $F_{vz'}$  are the forces parallel and normal to the PVC-s base-isolation interface induced by the vertical ground motion action  $F_v$ .

For the corresponding non-base-isolated school building, the numerical implementation is identical except for the boundary condition at the bottom is fixed to the natural ground, in which case the possible ground inclination has no effect to structural responses. In all models, with or without the PVC-s system, soil-structure interaction is not taken into consideration. A 5 % Rayleigh damping is employed based on the first two x-axis vibration modes of each numerical model.

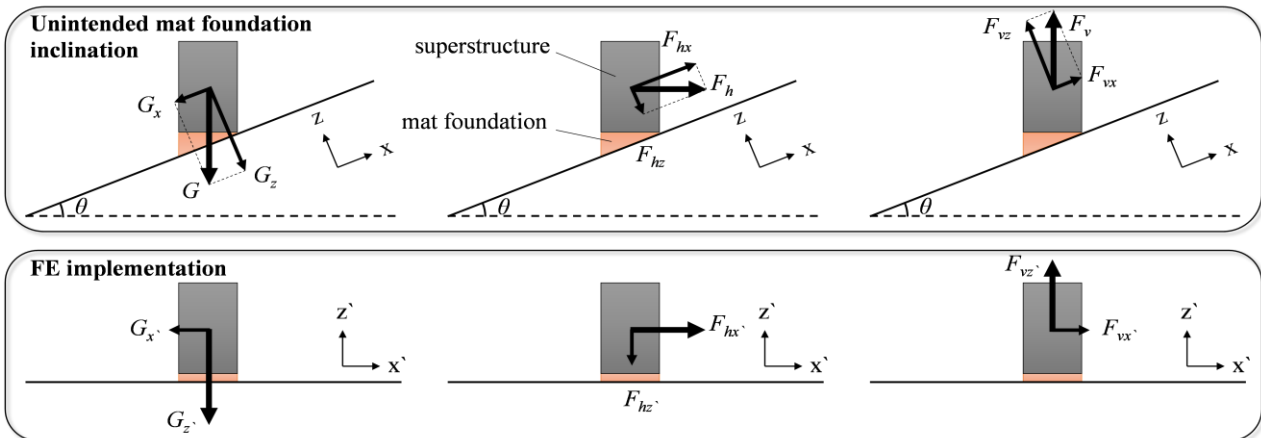


Figure 3: Illustration of finite element (FE) implementation of the unintended mat foundation inclination. Unintended PVC-s mat foundation inclination is assumed on x-axis only, where the building tends to slide down the negative x-direction.

### 2.3 Incremental Dynamic Analysis (IDA)

The 30 ground motions used in IDA (Vamvatsikos and Cornell, 2002) are identical as those delineated in (Sextos, Zhang and Alexander, 2022). They were selected from the PEER NGA-West 2 database (Ancheta *et al.*, 2013) assuming ground condition of Nepalese Soil Type A (roughly corresponds to Eurocode 8 Ground Type B or C). The selected ground motions contain three-axis acceleration excitation and the orientation-independent RotD100 component (Boore, 2006) of the two orthogonal horizontal components of the ground motion  $S_{a,h}(T_1)$  was used as the ground motion intensity measure (IM). According to Nepalese seismic design code (National Reconstruction Authority, 2020), the design-level elastic spectral acceleration of the case study school building can be calculated as 1.1 g. The scaling range of IM is chosen up to three times the design-level ground motion, i.e., up to 3.3 g.

The engineering demand parameter (EDP) of maximum storey one interstorey drift  $d_{storey1}$  is used to evaluate the seismic performance of the school building, as storey one (the ground floor) is where structural damage is found to be concentrated, thus thresholding the structural condition of the overall building. In addition, the effectiveness of the PVC-s base-isolation system is expressed as a drift reduction ratio  $D_{storey1}$ :

$$D_{storey1} = \frac{d_{storey1,Conventional} - d_{storey1,PVC-s}}{d_{storey1,Conventional}} \quad (7)$$

where  $d_{storey1,PVC-s}$  is the first storey maximum drift of the PVC-s base-isolated building; and  $d_{storey1,Conventional}$  is the first storey maximum drift of the corresponding conventional building. A higher value of  $D_{storey1}$  is beneficial as it implies a higher degree of seismic damage mitigation. For the sake of conducting statistical analysis, it is assumed that  $d_{storey1}$  follows lognormal distribution and  $D_{storey1}$  follows normal distribution, and all  $d_{storey1}$  values exceed 10 % are taken as 10 %. Damage states can be predicted based on  $d_{storey1}$ , which link descriptions of the building state with reference to certain  $d_{storey1}$  values. Various interstorey drift values were proposed in the literature to classify building damage states, especially predicting the collapse state, of which the corresponding storey drift values range from 2.5 % to 8.0 % for similar low-rise reinforced concrete moment resisting frames (Ghobarah, 2001, 2004; Liel and Deierlein, 2008; Haselton *et al.*, 2011; Uma *et al.*, 2011; Kassem, Mohamed Nazri and Noroozinejad Farsangi, 2020; Zhou *et al.*, 2021). Based on these references,  $d_{storey1} = 5.0\%$  is taken as the threshold of likely structural collapse in this study.

The sliding responses of the PVC-s base-isolated system are evaluated using two EDPs, namely, the maximum absolute PVC-s sliding displacement  $|\delta_{PVC-s,max}|$  and the PVC-s residual-to-maximum displacement ratio  $\Delta_{PVC-s,residual}$ . The former dictates whether pounding between the raft foundation and the sacrificial perimeter parapet wall would occur. Residual displacement is critical when assessing whether the building can be immediately operational after an earthquake event (including pre-shocks, the mainshock and aftershocks) or the utilities (such as water supply and drainage pipes, electricity connections) crossing the gap are damaged and need repair. Statistically, it is assumed that  $|\delta_{PVC-s,max}|$  follows lognormal distribution and  $\Delta_{PVC-s,residual}$  follows the two-parameter Beta distribution (Walck, 2007).

## 3 Numerical results

### 3.1 Time history responses

X- and y-axis time history responses of the PVC-s base-isolated school building subjected two earthquake ground motions, RSN1402 and RSN4850 (RSN: Record Sequence Number in the PEER NGA-West 2 database (Ancheta *et al.*, 2013)), are respectively given in Figure 4 and Figure 5. The ground motions are scaled so that the orientation-independent RotD100 component (Boore, 2006) of the two orthogonal horizontal components of the ground motion  $S_{a,h}(T_1)$  equals to 2.2 g, twice the design-level ground motion intensity calculated for the case study school building. Structural responses are represented in these figures using time histories of storey one interstorey drift  $\delta_{storey1}(t)$ , i.e., the red curves, whereas dynamic responses of the PVC-s base-isolation system is reflected by time histories of PVC-s system sliding displacement  $\delta_{PVC-s}(t)$ , i.e., the black curves. The results are presented comparatively between two cases of mat foundation inclination angle  $\theta$ , respectively,  $\theta = 0^\circ$  (the PVC-s base-isolation interface is perfectly level) and  $\theta = 3^\circ$  (the PVC-s base-isolation interface has extreme inclination due to mismanaged construction).

Under both ground motion excitations, the presence of unintended mat foundation inclination has resulted in increased foundation sliding displacements on the x-axis. During earthquakes, the sloping tends to increase

foundation sliding on the negative x-direction and prohibit those on the positive x-direction. Given the mat foundation inclination in addition to the known lack of any recentring capability for the PVC-s system, the maximum x-axis PVC-s sliding displacement changed from +0.051 m to -0.311 m for ground motion RSN1402 and from -0.091 m to -0.350 m for ground motion RSN4850. This is in line with engineering intuition, considering that the unintended mat foundation inclination is implemented in the finite-element models assuming sloping down the negative x-axis only. Nevertheless, it is also noted that the dynamic responses of the superstructure, in terms of interstorey drift, is not necessarily reduced nor increased due to mat foundation inclination. For ground motion RSN1402, the x-axis maximum absolute interstorey drift increases from 0.96 % to 1.07 % when  $\theta = 3^\circ$ , whereas for ground motion RSN4850 the response decreases from 2.38 % to 1.66 %. The moments at which interstorey drift maxima occur are found to be approximately the same, regardless of foundation inclination angle  $\theta$ .

On the other hand, it is noted that the y-axis responses of the PVC-s base-isolated school building are also strongly influenced by the assumed x-axis-only mat foundation inclination. Due to the inclination of PVC-s base-isolation interface within the x-z plane, variation of the force parallel to the PVC-s base-isolation interface in the x-z plane (i.e., the driving force of x-axis sliding) is dependent not only on the x-axis but the z-axis earthquake ground motion. In the same way, variation of normal contact force (i.e., the force governing the sliding threshold, on x- and y-axis) on the base-isolation interface is now also dependent on both the x- and z-axis earthquake ground motions. While the mechanism occurs in the x-z plane, the resultant variation on sliding threshold influences both the x- and y-axis dynamic responses of the base-isolated school building. For earthquake ground motion RSN1402, the maximum of interstorey drift  $\bar{\delta}_{storey1}(t)$  increased while the maximum of PVC-s sliding displacements  $\bar{\delta}_{PVC-s}(t)$  decreased. For ground motion RSN4850, the maximum of  $\bar{\delta}_{storey1}(t)$  decreased while the maximum of  $\bar{\delta}_{PVC-s}(t)$  increased but occurred on the other direction. It is believed that the influences of the above phenomena on seismic demand of the superstructure and on sliding behaviour of the PVC-s system are of random nature. At certain moments, the sliding threshold of the PVC-s system may be increased to the point beyond which a sliding action that would have occurred is now prohibited or delayed, leading to an increased instantaneous seismic demand on the superstructure, and vice versa.

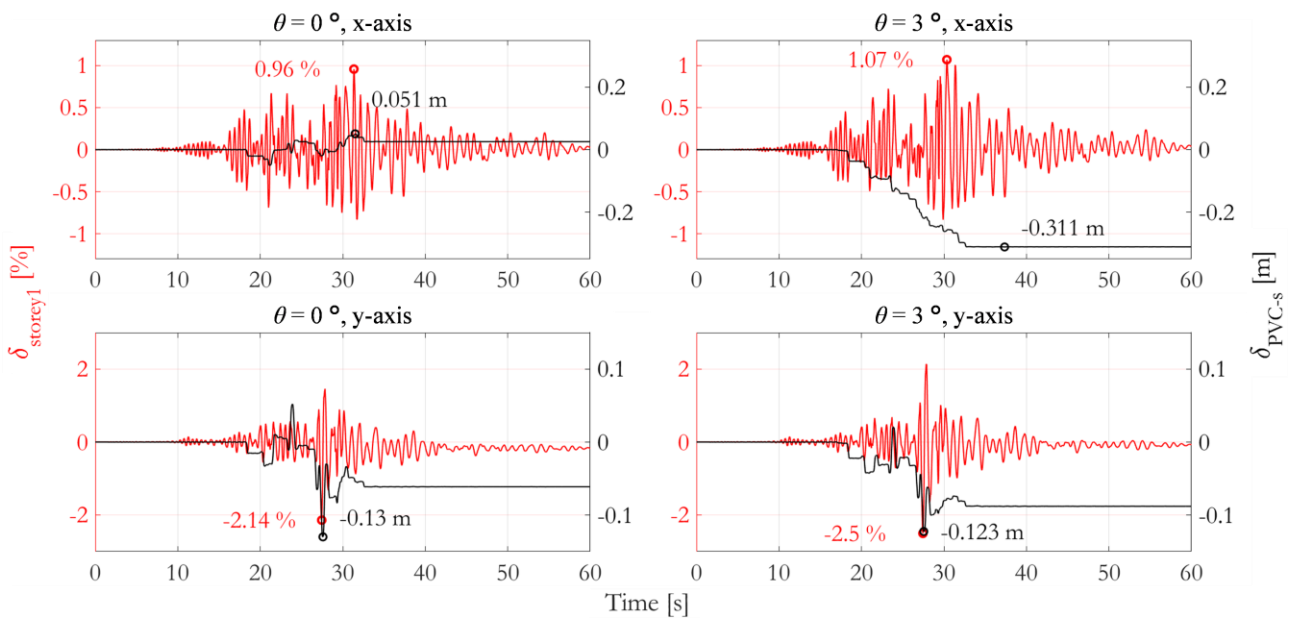


Figure 4: X- and y-axis time history responses of storey one interstorey drift  $\bar{\delta}_{storey1}$  [%] and PVC-s sliding displacement  $\bar{\delta}_{PVC-s}$  [m] for ground motion RSN1402 at intensity of  $S_{a,h}(T_1) = 2.2 g$ , given mat foundation inclination angles of  $\theta = 0^\circ$  or  $\theta = 3^\circ$ .

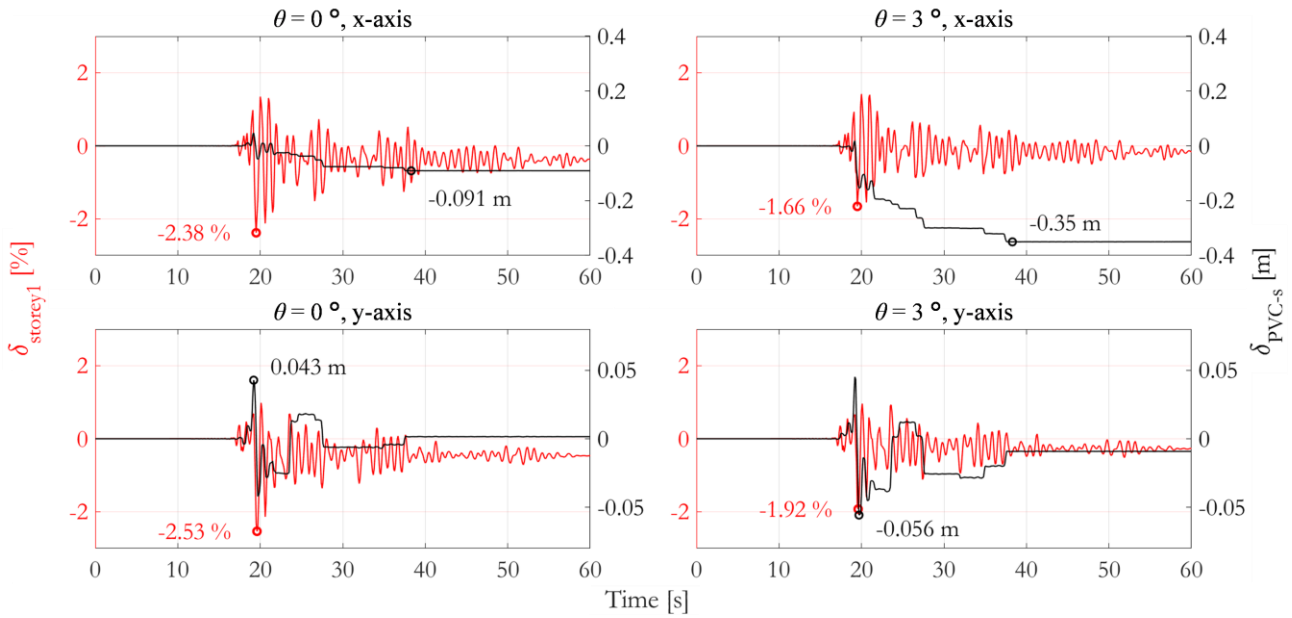


Figure 5: X- and y-axis time history responses of storey one interstorey drift  $\delta_{storey1}$  [%] and PVC-s sliding displacement  $\delta_{PVC-s}$  [m] for ground motion RSN4850 at intensity of  $S_{a,h}(T_1) = 2.2$  g, given mat foundation inclination angles of  $\theta = 0^\circ$  or  $\theta = 3^\circ$ .

### 3.2 Effect of mat foundation inclination on interstorey drift responses

The predicted  $d_{storey1}$  are very similar between the four PVC-s base-isolated buildings, regardless of the variation in  $\theta$ . This is quantitatively reflected, in Table 1, by the ratio of  $d_{storey1}$  values between one of the three non-zero  $\theta$  cases and the case  $\theta = 0$ , i.e.,  $d_{storey1,\theta > 0} / d_{storey1,\theta = 0}$ . It is found that the effectiveness of the PVC-s system is not necessarily improved or reduced for a ground motion given each  $S_{a,h}(T_1)$ - $\theta$  combination. From a probabilistic point of view, the average and median values of  $d_{storey1,\theta > 0} / d_{storey1,\theta = 0}$  under each  $S_{a,h}(T_1)$ - $\theta$  combination all closely approximate unity, meaning that the effect of unintended PVC-s system mat foundation inclination is statistically negligible.

Table 1: Ratio of storey one maximum interstorey drifts between cases with unintended PVC-s mat foundation inclination and the flat foundation case,  $d_{storey1,\theta > 0} / d_{storey1,\theta = 0}$  [%]. Colour in each cell represents the effect of unintended mat foundation inclination: red indicates foundation inclination reduces system effectiveness, green indicates foundation inclination benefits system effectiveness, yellow indicates cases where  $d_{storey1} > 10\%$  regardless of the foundation inclination angle  $\theta$ .

No. of GM	$S_{a,h}(T_1) = 1.1$ g			$S_{a,h}(T_1) = 2.2$ g			$S_{a,h}(T_1) = 3.3$ g		
	PVC-s, $\theta = 1^\circ$	PVC-s, $\theta = 2^\circ$	PVC-s, $\theta = 3^\circ$	PVC-s, $\theta = 1^\circ$	PVC-s, $\theta = 2^\circ$	PVC-s, $\theta = 3^\circ$	PVC-s, $\theta = 1^\circ$	PVC-s, $\theta = 2^\circ$	PVC-s, $\theta = 3^\circ$
1	117.0%	114.7%	120.2%	85.2%	102.6%	110.9%	92.5%	91.4%	88.2%
2	97.5%	97.3%	95.5%	98.5%	99.0%	106.4%	93.7%	95.7%	102.6%
3	97.1%	92.7%	91.1%	106.7%	103.4%	106.8%	112.7%	104.0%	99.9%
4	101.8%	101.9%	110.1%	104.2%	102.8%	104.0%	96.7%	87.0%	104.9%
5	105.1%	113.6%	121.4%	85.0%	80.4%	84.8%	111.3%	101.9%	102.5%
6	101.9%	104.2%	108.9%	87.0%	91.1%	97.2%	101.9%	89.4%	100.8%
7	104.4%	108.7%	110.9%	110.1%	104.3%	102.6%	78.9%	88.7%	89.8%
8	99.4%	101.2%	94.2%	89.9%	88.8%	96.0%	93.9%	102.6%	106.1%
9	102.9%	105.1%	101.1%	91.6%	97.5%	93.8%	107.9%	92.9%	102.9%
10	105.4%	103.3%	104.8%	104.3%	106.1%	86.0%	107.0%	112.0%	94.0%
11	97.3%	93.5%	95.5%	95.0%	101.3%	98.9%	97.4%	107.6%	106.0%
12	101.1%	101.3%	99.2%	99.4%	96.4%	96.0%	101.4%	97.7%	97.8%
13	94.6%	94.7%	93.9%	100.9%	105.7%	102.2%	92.2%	96.0%	92.7%
14	97.7%	93.8%	89.0%	92.4%	102.3%	105.3%	107.1%	99.8%	97.0%
15	94.7%	89.6%	84.6%	111.2%	131.5%	131.8%	83.2%	102.6%	98.5%
16	100.7%	95.6%	90.4%	128.0%	110.9%	121.4%	102.5%	104.7%	103.9%
17	97.0%	88.5%	93.9%	101.3%	117.0%	116.8%	110.5%	116.8%	126.5%
18	99.1%	97.1%	96.0%	97.0%	104.9%	93.1%	107.6%	95.4%	99.0%

19	103.2%	104.9%	106.6%	100.9%	101.1%	90.2%	105.0%	97.5%	101.3%
20	87.4%	100.3%	105.2%	102.7%	95.9%	75.1%	124.1%	112.8%	124.5%
21	101.0%	102.4%	98.9%	97.7%	99.2%	92.5%	97.9%	99.2%	104.1%
22	83.8%	93.4%	99.6%	N/A	N/A	53.2%	N/A	N/A	N/A
23	102.9%	103.5%	99.7%	101.5%	104.6%	102.0%	101.2%	102.6%	112.6%
24	100.2%	97.7%	92.8%	103.5%	105.6%	102.9%	103.3%	104.2%	105.5%
25	101.3%	101.9%	102.2%	109.6%	113.1%	114.3%	144.0%	149.3%	187.3%
26	104.9%	107.5%	119.1%	101.5%	107.1%	109.5%	N/A	N/A	N/A
27	102.6%	93.5%	96.8%	88.8%	100.6%	94.0%	97.7%	88.3%	102.4%
28	91.2%	113.9%	109.1%	N/A	N/A	N/A	N/A	N/A	N/A
29	100.7%	103.6%	113.7%	96.8%	104.6%	96.4%	106.1%	94.6%	99.7%
30	97.2%	101.1%	104.8%	104.9%	94.7%	107.9%	N/A	N/A	N/A
<b>Average</b>	99.7%	100.7%	101.6%	99.9%	102.4%	99.7%	102.6%	101.2%	105.0%
<b>Median</b>	100.7%	101.2%	99.6%	100.5%	102.4%	101.0%	101.3%	100.0%	101.1%

### 3.3 IDA curves

Results are statistically summarised by comparative IDA curves (Figure 6 to Figure 9) in the range of ground motion intensities up to  $S_{a,h}(T_1) = 3.3$  g (the vertical red dotted curves in the figures mark one-, two-, and three-time the design-level intensity). IDA curves are presented in terms of the four EDPs employed in this study, namely: the maximum storey one interstorey drift  $d_{storey1}$ , the drift reduction ratio  $D_{storey1}$ , the maximum absolute PVC-s sliding displacement  $|\delta_{PVC-s,max}|$ , and the PVC-s residual-to-maximum displacement ratio  $\Delta_{PVC-s,residual}$ .

The IDA curves of  $d_{storey1}$  (Figure 6) and  $D_{storey1}$  (Figure 7) are found to be effectively independent to the variation of  $\theta$  within the examined range of  $0^\circ \leq \theta \leq 3^\circ$ . Regardless of the variation on  $\theta$ , the reduction on seismic demand provided by the PVC-s system is evident, both at and beyond the design-level ground motion intensity. As an example, at  $S_{a,h}(T_1) = 3.3$  g, the probability of likely structural collapse is statistically estimated at 56 % for the conventional school building (i.e., without seismic base-isolation) and reduced to only around 27 % for its PVC-s base-isolated counterparts. It is also found that the effectiveness of the PVC-s base-isolation system is at its highest (median value of interstorey drift reduction  $D_{storey1} \approx 50$  %) between approximately 1.2 to 2.0 times the design-level ground motion intensity for the case study school building. The value of  $D_{storey1}$  can be always kept above 40 % for ground motions up to three times the design-level intensity. When the ground motion intensity is weaker than the design-level, seismically induced forces are expected to be safely withstood by the superstructure itself regardless of the existence of a seismic base-isolation system.

On the other hand, the presence of any unintended inclination on the PVC-s base-isolation interface strongly affects its sliding performance. It is found that the median value of  $|\delta_{PVC-s,max}|$ , as well as the associated statistical dispersion, tends to increase monotonically with respect to ground motion intensity  $S_{a,h}(T_1)$  (Figure 8). The  $|\delta_{PVC-s,max}|$  IDA curves also confirm that the reserved sliding gap of 0.35 m around the mat foundation is adequately realistic for PVC-s systems with no ( $\theta = 0^\circ$ ), moderate ( $\theta = 1^\circ$ ), or even significant ( $\theta = 2^\circ$ ) mat foundation inclinations. Under the circumstances of extreme mat foundation inclination ( $\theta = 3^\circ$ ), the median  $|\delta_{PVC-s,max}|$  can be factored by 2.5 to that of the flat-ground case and the probability of pounding between the mat foundation and the non-structural perimeter parapet wall is relatively high, around 24 % at  $S_{a,h}(T_1) = 2.2$  g and around 40 % at  $S_{a,h}(T_1) = 3.3$  g. Nevertheless, the effect of parapet wall pounding on the seismic demand of the main structure is expected to be negligible. This is because the parapet wall is a light, sacrificial element, of which the resistance to pounding is designed to be minimal.

When there is no mat foundation inclination ( $\theta = 0^\circ$ ), the PVC-s residual-to-maximum displacement ratio  $\Delta_{PVC-s,residual}$  (Figure 9) is characterised by median value of around 75 % with high statistical dispersion. The high dispersion can be attributed to the fact that the motion of a flat sliding system is reminiscent to a random walk. On the other hand, with the inclusion of mat foundation inclination, the values of  $\Delta_{PVC-s,residual}$  tend to increase towards unity and the dispersion tends to reduce. At extreme mat foundation inclination ( $\theta = 3^\circ$ ),  $\Delta_{PVC-s,residual}$  is almost always approximately 100 % with very little dispersion at and beyond the design-level ground motion intensity. This indicates that the foundation inclination is significant such that almost all sliding actions of the PVC-s system happen at the downward direction of the slope, whereas upward sliding is mostly prohibited. The phenomenon is in agreement with intuition, considering the fact that the PVC-s base-isolated building on an inclined mat foundation can be well represented by Newmark's analogy of sliding rigid block on frictional floor (Towhata, 2008), where the downward motion tends to be accumulated. This accumulation of downward motion can also be confirmed by the examples of x-axis sliding responses of the inclined PVC-s system as shown in Figure 4 and Figure 5.

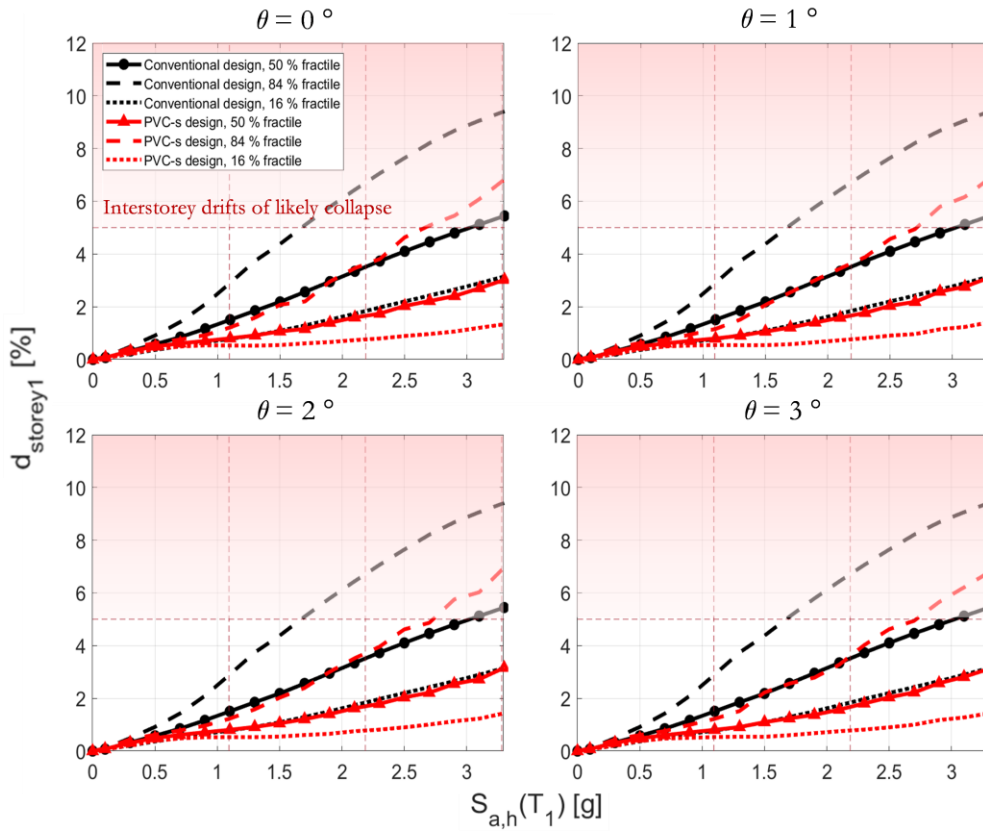


Figure 6: IDA curves (16 %, 50 % and 84 % fractiles) of maximum interstorey drifts of storey one  $d_{storey1}$  [%] for unintended mat foundation inclination angles  $\theta$  from  $0^\circ$  to  $3^\circ$ .

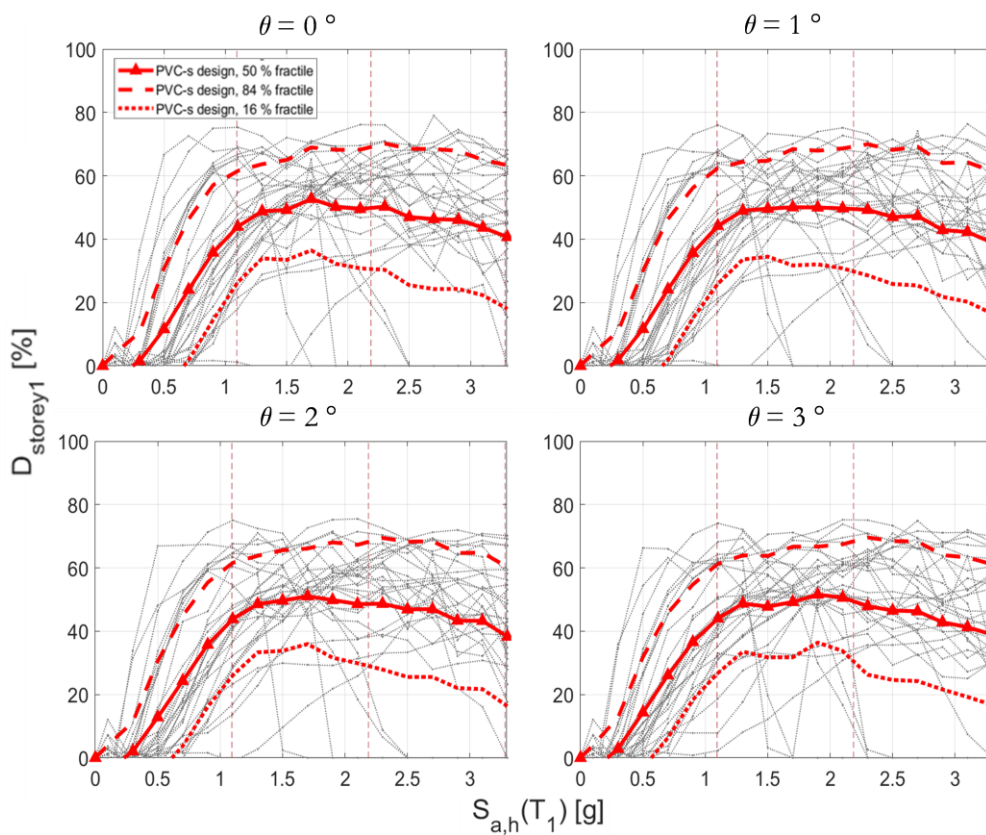


Figure 7: IDA curves (16 %, 50 % and 84 % fractiles) of storey one drift reduction ratio  $D_{storey1}$  [%] for unintended mat foundation inclination angles  $\theta$  from  $0^\circ$  to  $3^\circ$ .

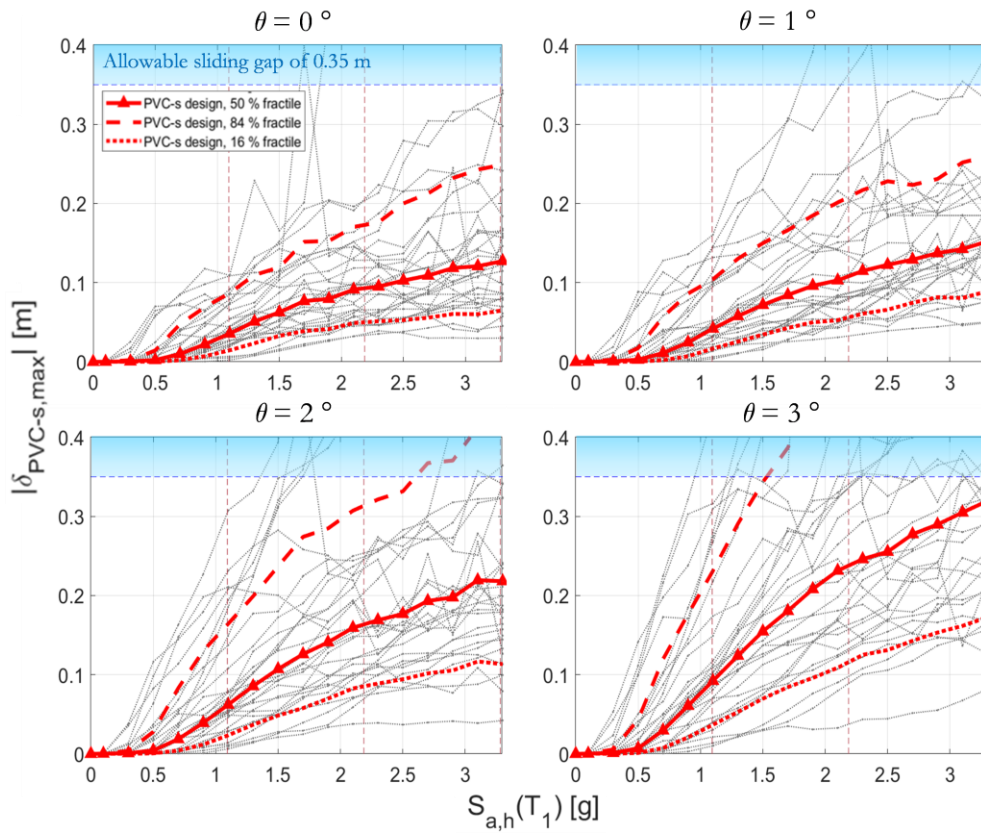


Figure 8: IDA curves (16 %, 50 % and 84 % fractiles) of maximum absolute PVC-s sliding displacement  $|\delta_{PVC-s,max}|$  [m] for unintended mat foundation inclination angles  $\theta$  from  $0^\circ$  to  $3^\circ$ .

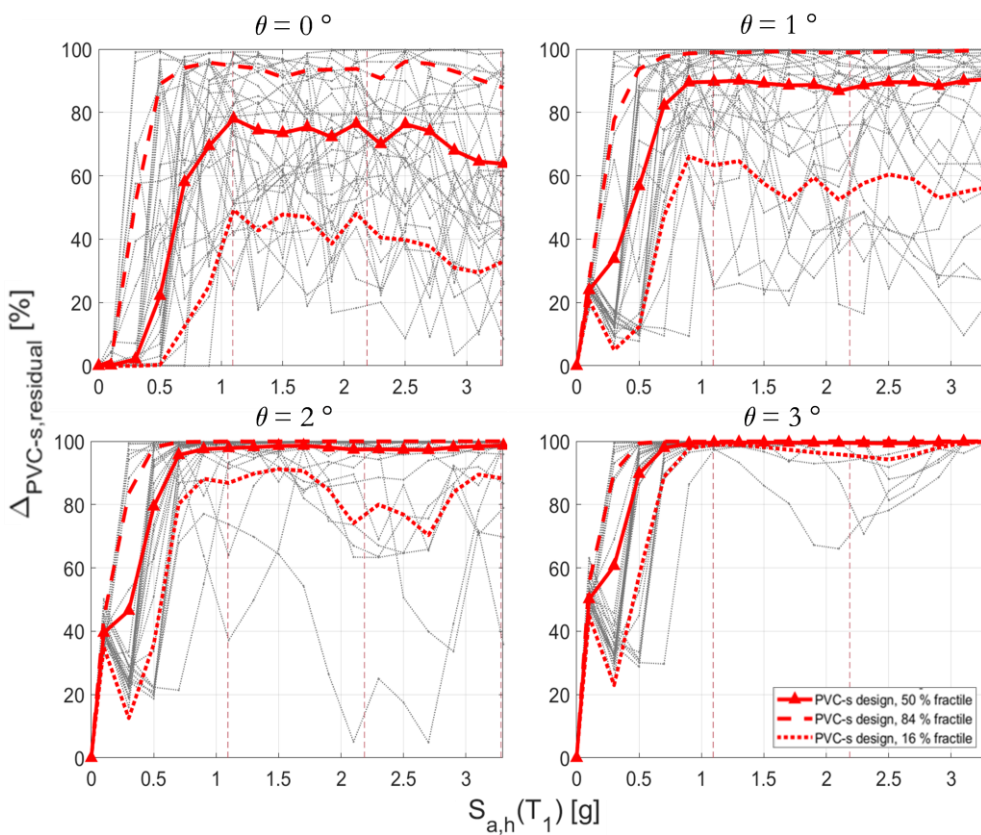


Figure 9: IDA curves (16 %, 50 % and 84 % fractiles) of PVC-s residual-to-maximum displacement ratio  $\Delta_{PVC-s,residual}$  [%] for unintended mat foundation inclination angles  $\theta$  from  $0^\circ$  to  $3^\circ$ .

## 4 Conclusions

The influence of a sloping seismic base-isolation interface, caused by unintended or mismanaged construction works, on the seismic performance of a typical Nepalese three-storey reinforced concrete school building protected by the low-tech, low-cost PVC 'sand-wich' (PVC-s) base-isolation system developed by the University of Bristol is investigated in this study. The effectiveness of the low-cost PVC-s base-isolation system is probabilistically verified for unintended mat foundation inclination angles up to 3 °. The following key observations are summarised:

- Performance of the low-cost, low-tech PVC-s base-isolation system is considered robust to probable unintended mat foundation inclinations, i.e., mat foundation inclination angle  $\theta \leq 3^\circ$ . By means of probabilistic Incremental Dynamic Analysis (IDA), it is found that unintended foundation inclination due to mismanaged construction works does not necessarily reduce nor increase the seismic demand on the superstructure, thus presenting very minimal statistical impact to the effectiveness of the PVC-s system.
- Displacement responses of the PVC-s system can be strongly affected by potential mat foundation inclination. Foundation sliding actions are more likely to occur on the downward direction, whereas upward sliding can be prohibited or delayed. As a result, the values of maximum PVC-s sliding displacement and its statistical dispersion tend to increase as the mat foundation inclination angle increases. The residual-to-maxima sliding displacement ratio also tends to get closer to unity. This issue cannot be self-mitigated by the PVC-s system since it is not designed to have recentring capabilities. Nevertheless, given the low-cost, low-tech nature of the PVC-s system, controlling sliding displacement is not regarded a primary concern in its typical usage scenario.
- The dynamic properties of the PVC-s base-isolated school building is altered by the existence of unintended mat foundation inclination in two aspects. The first aspect is the alteration of the forces that, respectively, govern the normal contact force on the PVC-sand-PVC sliding interface and drive potential foundation sliding on the sloping direction (in the x-z plane). The second aspect is the alteration of PVC-s system sliding threshold on all directions due not only to the vertical ground motion but also the horizontal acceleration aligning the sloping direction. The resultant dynamic interaction between responses parallel and perpendicular to the sloping direction is believed to be of random nature.

The PVC-s system is an efficient and robust alternative to some of the more high-tech seismic base-isolation technologies, particularly in cases where the latter cannot be applied widely for economic reasons. This study addressed the key question of how the critical construction defect of mat foundation inclination may influence the effectiveness of the PVC-s base-isolation system and proved that the system can be safely implemented for actual design and construction.

## 5 References

- Ancheta, T. et al. (2013) *PEER NGA-West2 Database, Technical Report PEER 2013/03*. California, USA. Available at: <https://ngawest2.berkeley.edu/site>.
- Boore, D.M. (2006) 'Orientation-Independent Measures of Ground Motion', *Bulletin of the Seismological Society of America*, 96(4A), pp. 1502–1511. Available at: <https://doi.org/10.1785/0120050209>.
- CEN (European Committee for Standardisation) (2004) *Eurocode 8: Design of structures for earthquake resistance - Part 1: General rules, seismic actions and rules for buildings*. Brussels: EN 1998-1:2004 (E).
- Ghobarah, A. (2001) 'Performance-based design in earthquake engineering: state of development', *Engineering Structures*, 23(8), pp. 878–884. Available at: [https://doi.org/10.1016/S0141-0296\(01\)00036-0](https://doi.org/10.1016/S0141-0296(01)00036-0).
- Ghobarah, A. (2004) 'On drift limits associated with different damage levels', in *International workshop on performance-based seismic design concepts and implementation*. Bled, Slovenia: Pacific Earthquake Engineering Research Center, pp. 321–332. Available at: [https://peer.berkeley.edu/sites/default/files/0405\\_edited\\_by\\_p.\\_fajfar\\_and\\_h.\\_krawinkler.pdf](https://peer.berkeley.edu/sites/default/files/0405_edited_by_p._fajfar_and_h._krawinkler.pdf).
- Giordano, N. et al. (2021) 'Financial assessment of incremental seismic retrofitting of Nepali stone-masonry buildings', *International Journal of Disaster Risk Reduction*, 60(May), p. 102297. Available at: <https://doi.org/10.1016/j.ijdrr.2021.102297>.

- Haselton, C.B. *et al.* (2011) 'Seismic Collapse Safety of Reinforced Concrete Buildings. I: Assessment of Ductile Moment Frames', *Journal of Structural Engineering*, 137(4), pp. 481–491. Available at: [https://doi.org/10.1061/\(ASCE\)ST.1943-541X.0000318](https://doi.org/10.1061/(ASCE)ST.1943-541X.0000318).
- Kassem, M.M., Mohamed Nazri, F. and Noroozinejad Farsangi, E. (2020) 'On the quantification of collapse margin of a retrofitted university building in Beirut using a probabilistic approach', *Engineering Science and Technology, an International Journal*, 23(2), pp. 373–381. Available at: <https://doi.org/10.1016/j.jestch.2019.05.003>.
- Kikuchi, M., Black, C.J. and Aiken, I.D. (2008) 'On the response of yielding seismically isolated structures', *Earthquake Engineering & Structural Dynamics*, 37(5), pp. 659–679. Available at: <https://doi.org/10.1002/eqe.777>.
- Liel, A.B. and Deierlein, G.G. (2008) *Assessing the Collapse Risk of California's Existing Reinforced Concrete Frame Structures: Metrics for Seismic Safety Desisions*. Stanford, California, USA. Available at: [https://stacks.stanford.edu/file/druid:zb577jt6355/TR166\\_Liel.pdf](https://stacks.stanford.edu/file/druid:zb577jt6355/TR166_Liel.pdf).
- National Reconstruction Authority (2020) *Seismic Design of Buildings in Nepal, Ministry of Urban Development*. Babar Mahal, Kathmandu, Nepal: NBC 105: 2020.
- Seismosoft Ltd. (2022) *SeismoStruct User Manual*. Pavia, Italy.
- Sextos, A.G., Zhang, Z. and Alexander, N.A. (2022) 'Large-Scale Testing for Enhancing the Resilience of Schools in Seismic Regions: Challenges and Cost-Efficient Solutions', in R. Vacareanu and C. Ionescu (eds) *Progresses in European Earthquake Engineering and Seismology – Third European Conference on Earthquake Engineering and Seismology – Bucharest, 2022*. Springer International Publishing (Springer Proceedings in Earth and Environmental Sciences), pp. 433–448. Available at: [https://doi.org/10.1007/978-3-031-15104-0\\_26](https://doi.org/10.1007/978-3-031-15104-0_26).
- Towhata, I. (2008) *Geotechnical Earthquake Engineering*. Edited by W. Wu and R.I. Borja. Springer, Berlin, Heidelberg. Available at: <https://doi.org/10.1007/978-3-540-35783-4>.
- Tsiavos, A. *et al.* (2019) 'A sand-rubber deformable granular layer as a low-cost seismic isolation strategy in developing countries: Experimental investigation', *Soil Dynamics and Earthquake Engineering*, 125(June), p. 105731. Available at: <https://doi.org/10.1016/j.soildyn.2019.105731>.
- Tsiavos, A. *et al.* (2020) 'Large-scale experimental investigation of a low-cost PVC "sand-wich" (PVC-s) seismic isolation for developing countries', *Earthquake Spectra*, 36(4), pp. 1886–1911. Available at: <https://doi.org/10.1177/8755293020935149>.
- Tsiavos, A., Sextos, A., Stavridis, A., Dietz, M., Dihoru, L. and Alexander, N.A. (2021) 'Experimental investigation of a highly efficient, low-cost PVC-Rollers Sandwich (PVC-RS) seismic isolation', *Structures*, 33(May), pp. 1590–1602. Available at: <https://doi.org/10.1016/j.istruc.2021.05.040>.
- Tsiavos, A., Sextos, A., Stavridis, A., Dietz, M., Dihoru, L., Di Michele, F., *et al.* (2021) 'Low-cost hybrid design of masonry structures for developing countries: Shaking table tests', *Soil Dynamics and Earthquake Engineering*, 146(June 2020), p. 106675. Available at: <https://doi.org/10.1016/j.soildyn.2021.106675>.
- Uma, S.R. *et al.* (2011) 'Comparison of main-shock and aftershock fragility curves developed for New Zealand and US buildings', in *9th Pacific Conference on Earthquake Engineering*. Auckland, New Zealand, pp. 1–9. Available at: <http://www.nzsee.org.nz/db/2011/227.pdf>.
- Vamvatsikos, D. and Cornell, C.A. (2002) 'Incremental dynamic analysis', *Earthquake Engineering & Structural Dynamics*, 31(3), pp. 491–514. Available at: <https://doi.org/10.1002/eqe.141>.
- Vassiliou, M.F., Tsiavos, A. and Stojadinović, B. (2013) 'Dynamics of inelastic base-isolated structures subjected to analytical pulse ground motions', *Earthquake Engineering & Structural Dynamics*, (056), pp. 1–18. Available at: <https://doi.org/10.1002/eqe.2311>.
- Walck, C. (2007) *Hand-book on Statistical Distributions for Experimentalists, Internal Report SUF-PFY/96-01*. University of Stockholm, Stockholm, Sweden.
- Zhou, J. *et al.* (2021) 'Challenges in Evaluating Seismic Collapse Risk for RC Buildings', *International Journal of Concrete Structures and Materials*, 15(1), p. 27. Available at: <https://doi.org/10.1186/s40069-021-00463-y>.